

Detecting Faults in Doubly Fed Induction Generator by Rotor Side Transient Current Measurement

Goran Stojcic, Kenan Pasanbegovic

Department of Energy Systems and Electrical Drives
Vienna University of Technology
Vienna, Austria
goran.stojcic@tuwien.ac.at

Thomas M. Wolbank

Department of Energy Systems and Electrical Drives
Vienna University of Technology
Vienna, Austria

Abstract—The doubly fed induction generator (DFIG) is one of the main technologies at variable speed power generation systems. Reliability and efficiency are key factors to realize the maximum energy output of the renewable resources. Detecting generator faults enables the reduction of risk for unexpected outages and thus high economic losses. Stator winding insulation faults count to one of the most frequent failures in electric machines. Common fault detection methods are based on several additional sensors and hardware what makes the system complex, expansive and also fault-prone. In this work a method is proposed and investigated to detect stator winding faults based only on measured signals available from inverter build-in sensors. By rotor-side inverter switching the generator is excited by transient voltage pulses and the current response provides the possibility to extract a fault indicator through a specific signal processing. Measurements on DFIG test stand prove the methods applicability and accuracy.

I. INTRODUCTION

Increasing power generation based on renewable energy sources has raised the application of doubly fed induction generator (DFIG). Mainly used in wind turbine and pump-storage applications the DFIG has become a key component. The generator may be subject to different sort of failures and unexpected outages and downtime can lead to high economic losses. Thus, condition monitoring of the generator is mandatory to meet the demands of reliable and cost efficient power generation. Identification of electromechanical generator faults already in an early stage is highly appreciated to enable emergency operation and reduce the risk of catastrophic damages. Detecting faults already in their developing state can provide the possibility to react timely and can prevent from complete destruction of generator or entire system. On the other hand the maintenance efforts can also be reduced by detecting the fault in a very early stage. Monitoring sequences can be carried out periodically and the knowledge of machine state is permanently accessible without the need of reduced maintenance intervals or additional sensors and evaluation systems. Much work has

been done in academia as well as industry in this topic [1],[3],[4]. However, most of the methods are based on additional sensors, what makes the condition monitoring and fault detection systems extremely expensive and complex [1]. Another drawback is given by the fact that these sensors are also prone to defects and may lead to additional downtimes. Therefore methods have to be developed based only on electrical machine quantities as stator/rotor current or voltage to reduce the complexity of the monitoring system. In recent time some methods have been published [1]-[16] dealing with the issue of detecting faults only by generator current and voltage signals. Most of these methods are based on frequency analysis by Fourier transform [6]-[10]. An improvement of these methods can be found in [11]-[13] but having the drawback of high computational costs. Furthermore all these methods have to deal with the impact of closed-loop drive systems as they arise from open-loop applications.

This work presents a method enabling detection of incipient faults in DFIG based only on the electrical quantities of rotor and stator. The main advantage is given by the usage of only current sensors of the rotor as well stator that are already present in the control system. Exploiting switching transients of the rotor side inverter provides the possibility to develop a fault indicator for detecting fault induced machine asymmetries. As the rotor is excited by short voltage pulses impacts of closed-loop effects are avoided and the signal processing procedure is kept on a low level using only basic mathematical functions. Thus the presented method can be applied to existing systems easily, considering not only floating point but also fixed point operation processors in the control system.

II. ESTIMATION OF TRANSIENT LEAKAGE INDUCTANCE

The main idea is to exploit the machine response to transient excitation. Short voltage pulses applied by inverter switching to machine terminals will evoke a current response which is dominated by the transient leakage inductance.

Comparing the current responses of different phases provides the information on machine's state and asymmetries. It has to be mentioned that in the following description a restriction is made to a specific operation state: rotor winding fed by inverter and the stator winding is short-circuited by an external switch. This is a common start up procedure for doubly fed induction generator applications [1].

Assuming now a symmetrical machine, electrical behavior can be written from rotor side as:

$$\underline{v}_R = r_R \cdot \underline{i}_R + l_I \cdot \frac{d\underline{i}_R}{d\tau} + \frac{d\underline{\lambda}_S}{d\tau} \quad (1)$$

An applied voltage phasor \underline{v}_R generated by any of the active inverter output states leads to a transient current change $d\underline{i}_R/d\tau$. This current change is influenced by different parameters. Besides the leakage inductance l_I also the voltage drop $r_R \underline{i}_R$ as well as the electromotive force (back emf) from the stator $d\underline{\lambda}_S/d\tau$, the dc link voltage and the inverter output state will influence the current change. After applying a voltage step by inverter switching from inactive to any active state the first current reaction will be dominated by the leakage inductance and the back emf. To enable an accurate identification of the leakage inductance the disturbing back emf has to be eliminated. A simple but very effective way is to apply two short voltage pulses of some μs duration with opposite direction. Due to the short pulse duration the back emf as well as the dc link voltage and fundamental-wave current \underline{i}_S can be assumed constant. Within each pulse duration (1) can be set up individually. Elimination of disturbing voltage drops is then realized by subtraction of both pulse equations as shown in (2) (index I for the first and II for the second pulse, respectively). As the excitation is transient the actual leakage inductance is additionally denoted as the transient leakage inductance $l_{I,t}$ which differs from the fundamental-wave leakage inductance.

$$\begin{aligned} \underline{v}_{R,I} - \underline{v}_{R,II} &= \overbrace{r_R \cdot \underline{i}_{R,I} - r_R \cdot \underline{i}_{R,II}}^{\approx 0} + l_{I,t} \cdot \frac{d\underline{i}_{R,I}}{d\tau} - \\ &l_{I,t} \cdot \frac{d\underline{i}_{R,II}}{d\tau} + \underbrace{\frac{d\underline{\lambda}_{S,I}}{d\tau} - \frac{d\underline{\lambda}_{S,II}}{d\tau}}_{\approx 0} = \\ &l_{I,t} \cdot \left[\frac{d\underline{i}_{S,I}}{d\tau} - \frac{d\underline{i}_{S,II}}{d\tau} \right] \end{aligned} \quad (2)$$

Considering now a real machine, faulty or not the transient inductance will no more be a scalar but a spatial complex value $\underline{l}_{I,t}$. This results from the fact that the direction of the voltage difference phasor $\underline{v}_{R,I-II} = (\underline{v}_{R,I} - \underline{v}_{R,II})$ and the current derivative difference phasor $d\underline{i}_{R,I-II}/d\tau = (d\underline{i}_{R,I}/d\tau - d\underline{i}_{R,II}/d\tau)$ will no longer be aligned.

This complex transient leakage inductance can now be portioned into two parts, an 'offset' part and a 'mod'

(modulated) part (3). The scalar offset part l_{offset} represents the symmetrical machine while the complex modulation part l_{mod} the fault induced asymmetries.

$$\begin{aligned} \underline{l}_{I,t} &= l_{offset} + l_{mod} \\ l_{mod} &= l_{mod} \cdot e^{j2\gamma} \end{aligned} \quad (3)$$

As given in (2), measuring of the resulting current slope is sufficient to calculate the angular position of the maximum inductance. This can be done if (3) is inserted in (2) and inverted; what leads to (4) with $\underline{y}_{I,t} = 1/\underline{l}_{I,t}$.

The voltage difference phasor $\underline{v}_{R,I-II}$ can be assumed constant during each measurement period. This leads to the simplification $d\underline{i}_{R,I-II}/d\tau \sim \underline{y}_{I,t}$, thus it is clear that observing only the current derivative difference phasor is sufficient for transient leakage inductance estimation. Furthermore the number of executed mathematical operations in real time is reduced to a minimum, as only current sampling is needed.

$$\frac{d\underline{i}_{R,I-II}}{d\tau} = \underline{y}_{I,t} \cdot \underline{v}_{R,I-II} = [\underline{y}_{offset} + \underline{y}_{mod}] \cdot \underline{v}_{R,I-II} \quad (4)$$

With this coherence the measured current derivative difference phasor $d\underline{i}_{R,I-II}/d\tau$ can also be portioned as shown in (4). The offset part is pointing in the direction of the voltage difference phasor $\underline{v}_{R,I-II}$. On the other hand the modulated part now is dependent on the direction of the maximum inductance. Hence, the modulated part of the current derivative difference phasor provides information on machine asymmetries.

III. FAULT INDICATOR CALCULATION BY SIGNAL PROCESSING

As stated in the previous section, by estimating the current derivative difference phasor the transient leakage inductance information of generator's state can be acquired and used to detect asymmetries. However, to achieve this detection, some specific signal processing steps have to be performed. In a first step the symmetrical portion of $d\underline{i}_{R,I-II}/d\tau$ has to be eliminated. Realizing the voltage difference phasor sequence such, that it consists of two phasors pointing in opposite direction of one phase and applying the sequence to the three main phase directions of the rotor also three current derivative difference phasors are obtained. The symmetrical portion of each current derivative difference phasor then points into the corresponding main phase direction. Adding up all three current derivative difference phasors leads to only one resulting phasor and the symmetrical portion being removed as zero sequence component. The remaining phasor now only depends on the machine's asymmetries and is denoted asymmetry phasor in the following. In a real machine even faultless, there are always some inherent asymmetries present. These asymmetries are detectable and

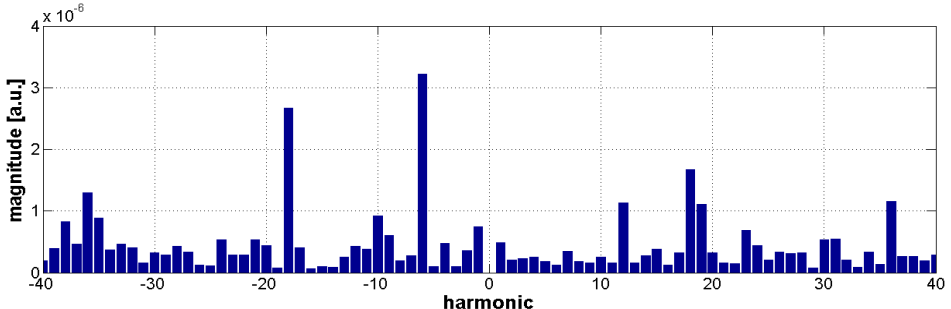


Fig. 1: Harmonic asymmetry phasor content of the investigated DFIG

separable due to their deterministic behavior leading to modulation of the asymmetry phasor when the inherent asymmetries spatially move. To achieve an accurate fault indicator signal they have thus to be eliminated. The main reasons for inherent asymmetries are given by winding distribution, slotting and anisotropy. The Fast Fourier Transformation (FFT) provides an effective possibility to separate their modulations from the asymmetry phasor signal. It is however necessary to collect a set of asymmetry phasors clearly showing the different inherent asymmetry's modulations. This collection can be established by a specific measuring sequence as follows. In a first step the voltage pulse sequences are applied to all three main phase directions and by measurement of the current signal and subsequent signal processing the asymmetry phasor is obtained as described above. In the next stage the rotor is moved and the data acquisition is repeated, at least a phasor set for one slotting period must be acquired. As already mentioned the method is intended for the very first stage of the start-up or black-start operation of variable speed generator systems. Therewith the rotor movement is realized by the turbine or auxiliary equipment. Ensuring a high quality and accurate signal processing and fault indicator generation the asymmetry phasor set was collected for one mechanical revolution in this investigation.

The spectral content of the machine investigated in this work is given in Fig. 1. As the asymmetry phasors are complex values the resulting spectrum also is of complex nature. As can be seen, several harmonics are dominant in the spectrum. The main harmonics are the -6^{th} , $+12^{\text{th}}$, $\pm 18^{\text{th}}$ and $\pm 36^{\text{th}}$. The stator of the present machine has 36 stator slots and 3 pole pairs and thus the $\pm 36^{\text{th}}$ harmonic is related to this parameter. The -6^{th} harmonic results from a combination of magnetic iron core properties and winding distribution and the $\pm 18^{\text{th}}$ and $+12^{\text{th}}$ as higher harmonics of the non-sinusoidal winding modulations. Assuming now a stator related fault (e.g. incipient open-circuit fault, turn-to-turn fault) the electromagnetic properties of the stator winding changes and thus also the transient leakage inductance. Considering now a fault at a certain stator position this will induce an asymmetry equal to the number of poles when moving the rotor for one full mechanical revolution. For the investigated machine this will be the -6^{th} harmonic due to 6 poles. So, a fault induced asymmetry will be detectable in this harmonic and will be denoted as fault

indicator. Considering a defect in the rotor, the asymmetry is fixed with the rotor related frame. Thus the harmonic to be observed for such fault cases is the offset. For a clearer presentation of the signal processing Fig. 2 shows a block diagram.

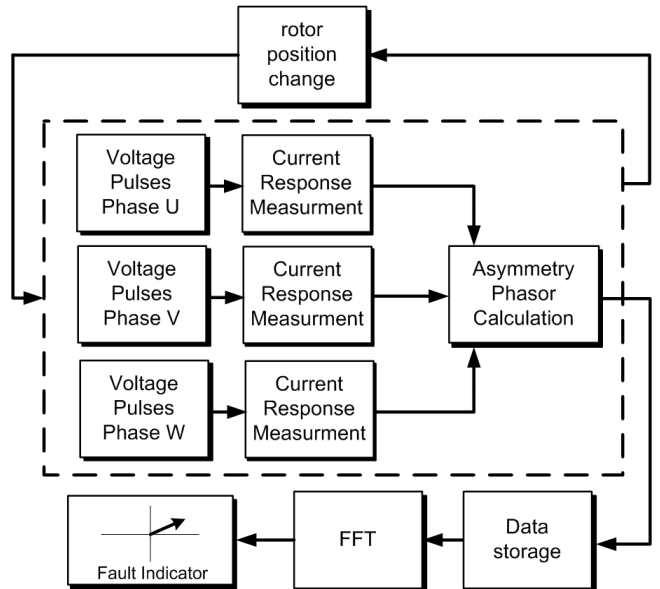


Fig. 2: Block diagram of signal processing for fault indicator generation

IV. EXPERIMENTAL VERIFICATION BY MEASUREMENTS

A. Test Stand Setup

To prove the methods applicability an experimental test stand was set up as presented in Fig. 3. The test machine (DFIG) is a 6 pole 10.3kW induction machine with wound rotor and slip ring connectors. The stator has 36 slots and the rotor 54 slots. A voltage source inverter is connected to the slip rings and serves as rotor side inverter. The dc link voltage is 440V. A variable speed induction machine (IM) is operated through an ac-to-ac inverter system and can be controlled by a computer system. This system is the drive unit to realize the rotor movement of the DFIG. The control and measurement system is realized by a computer system programmable under MATLAB/Simulink. The test machine stator can be connected to main supply, short circuited or the machine can be operated under isolated load. This is indicated by a switch in Fig. 3. To ensure the applicability of

the proposed method only sensors are used for the calculation of the fault indicator that are also present in standard industrial and power generation systems (rotor current, shaft speed).

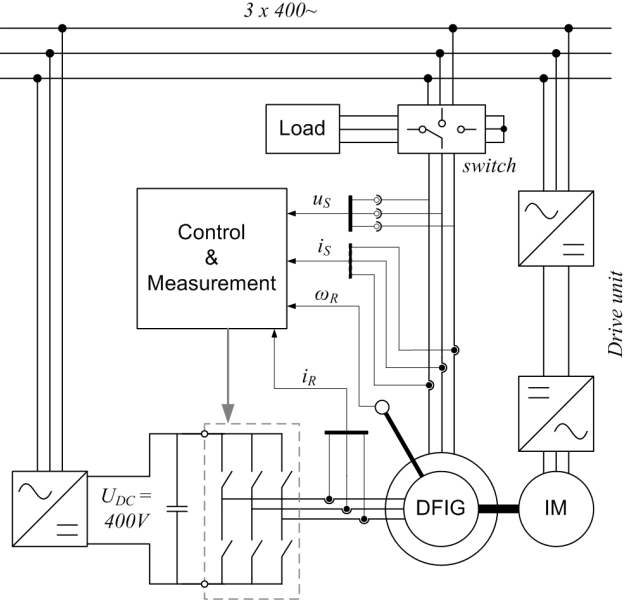


Fig. 3: Scheme of the DFIG test stand

B. Symmetrical machine

In a first step the machine was investigated under symmetrical conditions. Therefore the stator was short-circuited by an external switch and the rotor was slowly moved by the drive unit. This state is common in the very first period of a DFIG during start up [1]. The measurements were carried out as described in the previous section.

In Fig. 5 the harmonic content of the asymmetry phasor set obtained by the measurement is presented. In the upper diagram the rotor side, in the lower diagram the stator side. All the values are given in arbitrary units [a.u.] according to the signal processor internal representation. The calculation of the fault indicator described in the previous section was based on the rotor side current sensors only. Nevertheless, this can be also executed for the stator side. Thereby the stator current response due to the voltage pulses applied by the rotor side inverter is measured. The calculation is executed in the very same way but with the current derivative difference phasor $d\dot{i}_{S,LII}/d\tau$ estimated by the stator current measurement. Fig. 4 and Fig. 5 are presenting the real part and the harmonic content of the obtained asymmetry phasor set. The machine was operated with zero flux and no load and the stator side was short circuited by an external switch (compare Fig. 3). The drive unit was moving the rotor with 5% of nominal speed. Comparing the spectra of rotor and stator side the +6th harmonic in the stator related spectrum is more dominant. This modulation is linked with the number of poles (6 for the test machine). The -6th is almost equal in both diagrams.

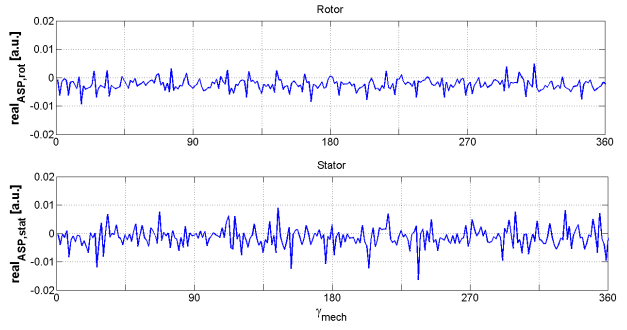


Fig. 4: Real part of the asymmetry phasor set. The current response measurement was performed on the rotor ($\text{real}_{ASP,\text{rot}}$) and stator ($\text{real}_{ASP,\text{stat}}$) side. Machine state: stator short-circuited, symmetrical.

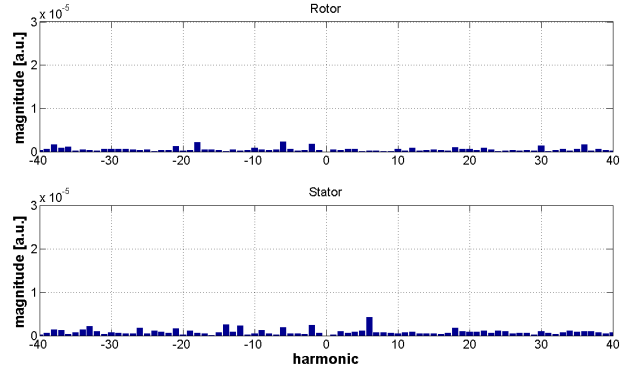


Fig. 5: Harmonic content of the asymmetry phasor set. The current response measurement performed on the rotor and stator side. Machine state: stator short-circuited, symmetrical.

C. Stator Related Faults

The most frequent faults considering electrical machines are stator related faults. Emulation of such fault cases can be realized by connecting an additional inductance (L_{add}) in series with a stator phase. Thus an asymmetry in the stator system is generated comparable to an asymmetry induced by a stator fault as a turn-to-turn short-circuit. The value of L_{add} was tuned to induce a stator asymmetry compared to a stator turn-to-turn short-circuit induced asymmetry in a squirrel cage inductance machine. The measurement procedure and fault indicator estimation calculations were executed as described for the symmetrical case. To ensure equal conditions as for the previous case the rotor speed was set to 5% nominal value and the stator was short-circuited by an external switch. The real portion of the asymmetry phasor set signal and the harmonic content of the signal obtained by this measurement is given in Fig. 6 and Fig. 7, respectively. It can be clearly seen that the rotor side real portion signal contains a modulation with a period of 6 corresponding to the mechanical angle γ_{mech} . This can be also observed on the stator side spectrum but with reduced amplitude. In the spectral presentation the difference between stator and rotor side of the -6th harmonic is more visible. Based on these measurements it can be stated that fault detection can be based on the stator or rotor side current measurement. However, fault indicator calculation is based on the rotor

side due to the dominant increase of the rotor side -6th harmonic and thus an improved signal-to-noise ratio.

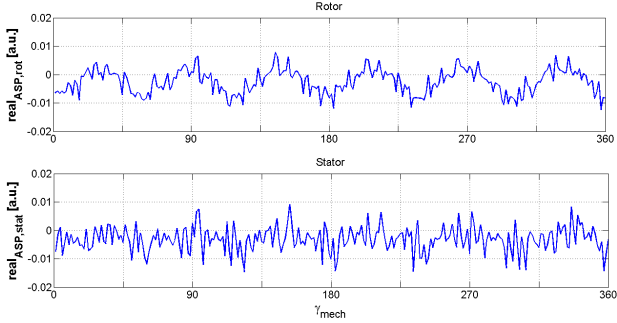


Fig. 6: Real part of the asymmetry phasor set. The current response measurement was performed on the rotor (real_{ASP,rot}) and stator (real_{ASP,stat}) side. Machine state: stator short-circuited, symmetrical.

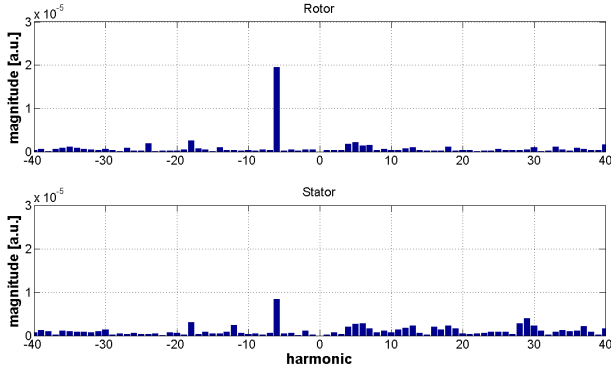


Fig. 7: Harmonic content of the asymmetry phasor set. The current response measurement performed on the rotor and stator side. Machine state: stator short-circuited, additional inductance L_{add} in phase U.

D. Stator fault detection accuracy

As the fault indicator obtained from the measurements and calculation is of complex nature, not only asymmetry magnitude (i.e. harmonic content) but also its direction can be identified. The fault indicator can be considered as a phasor in the complex plane pointing in direction of the faulty phase. In Fig. 8 the fault indicator results are shown for several cases. The red star is corresponding to the faultless case located in the origin of the complex frame. In addition it must be mentioned that an offset is present even for the faultless machine representing stator fixed asymmetries like anisotropy and measurement equipment (sensors, wiring) imperfections. By pre-commissioning this portion can be eliminated, so done in the present diagram. It has to be mentioned that according to (4) the current derivative difference phasor $d\dot{I}_{R,I-II}/d\tau$ proportional to $\underline{y}_{l,t}$. is used as input for the fault indicator. Thus an inversion is introduced in the signal processing chain (a bigger inductance leads to lower $d\dot{I}_{R,I-II}/d\tau$). Thus the phase arrows in Fig. 8, Fig 9 point in negative phase direction.

By placing L_{add} in phase U the fault indicator (green cross) is moving towards phase direction U indicated by a black arrow. Removing the additional inductance from phase U and connecting to phase V the fault indicator is also

changing the position into direction V (magenta cross). In the next step the additional inductance is connected in phase V and phase W simultaneous. The fault indicator (blue cross) is pointing into negative U direction. Therewith confusion with phase U faults can be excluded by considering the fault indicator direction. To analyze the methods accuracy the inductance connected to phase U was reduced to 0.5·L_{add} and 0.25·L_{add}. The obtained results for these measurements are presented by cyan and black cross, respectively. The fault indicator magnitude is reduced at the same ratio as the inductance value but the direction is still the same. All cases are denoted by the fault severity and phase where the asymmetry is located.

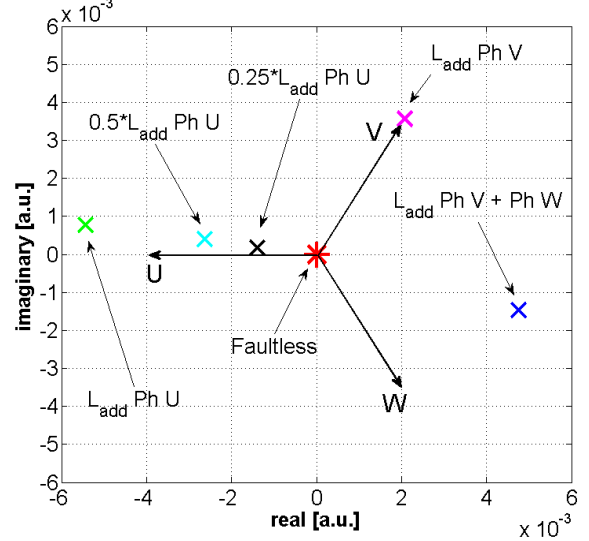


Fig. 8: Fault indicator measurement results for faultless case and different stator related fault cases.

E. Rotor Related Faults

Beside the stator related faults also rotor winding faults count to frequent faults considering wound rotor machines. As the transient leakage inductance is influenced by the stator as well rotor side, also rotor related faults can be identified. Therefore, the fault indicator estimation must be adapted due to the fact that the excitation is fixed with rotor windings. Assuming a fault in the rotor windings the faulty position is also moving with the rotor. Thus the fault induced harmonic of the fault indicator is not equal the pole pair as for stator related faults but the offset component. So, the measurement procedure and signal processing presented in Fig. 2 remains the same and but the fault indicator is now the offset portion.

Verification of fault detection applicability and accuracy was realized as for the stator related faults by connecting an additional inductance in series with one phase. Several fault cases and measurements were performed. In Fig 9 all the results are presented as fault indicator in the complex plane. The fault severities and positions were chosen equal to the stator fault emulation. At first, the symmetrical machine was investigated. The stator was short-circuited by the external switch and the rotor speed set again to 5% nominal value. The fault indicator result is located again in the origin of the

complex plane (red star). In the next step L_{add} was connected in series to phase U following by reduction of L_{add} in two steps by 50% and 75%. The fault indicator for all three fault cases (green, cyan and black cross) clearly points in phase direction U and the magnitude is decreasing with lower asymmetry values. In the last two cases L_{add} was connected to phase V and W, respectively (magenta and blue cross). Thus the direction correlation of fault indicator and fault position is proved.

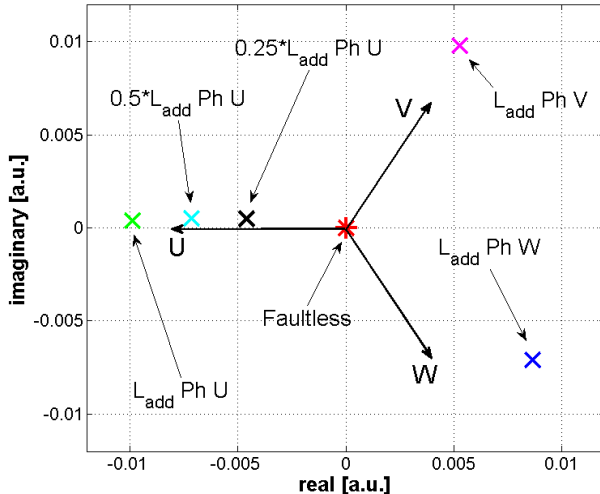


Fig 9: Fault indicator measurement results for faultless case and different rotor related fault cases.

V. CONCLUSION

The technique presented in this paper allows the detection of stator and rotor related asymmetries in the winding system of doubly fed induction generators. Applying short voltage pulses of some ten μs duration to the machine terminals and measuring the current reaction provides the knowledge of the machine's transient leakage inductance. By a special signal processing procedure a fault indicator is developed to identify stator asymmetries by using the rotor side inverter built-in current sensors only. Asymmetries can be detected with their severity as well as position. A special test stand with a slip ring induction machine and a drive unit was set up to prove the methods applicability and accuracy. The asymmetry emulation was realized by connecting additional inductances with different values in series with the stator phases. Measurements for different fault scenarios have shown satisfactory results when detecting asymmetries

ACKNOWLEDGMENT

The work to this investigation was supported by the Austrian Science Fund (FWF) under grant number P23496-N24.

REFERENCES

- [1] Daneshi-Far, Z.; Capolino, G.A.; Henao, H.; "Review of failures and condition monitoring in wind turbine generators" *Electrical Machines (ICEM), 2010 XIX International Conference on*, vol., no., pp.1-6, 2010
- [2] Bin Lu; Yaoyu Li; Xin Wu; Zhongzhou Yang; "A review of recent advances in wind turbine condition monitoring and fault diagnosis" *IEEE Power Electronics and Machines in Wind Applications, 2009. PEMWA 2009*, vol., no., pp.1-7, 2009
- [3] Wilkinson, M.R.; Spinato, F.; Tavner, P.J.; "Condition Monitoring of Generators & Other Subassemblies in Wind Turbine Drive Trains" *IEEE International Symposium on Diagnostics for Electric Machines, Power Electronics and Drives, 2007. SDEMPED 2007*, , vol., no., pp.388-392, 2007
- [4] Z. Hameed, Y.S. Hong, Y.M. Cho, S.H. Ahn, C.K. Song, "Condition monitoring and fault detection of wind turbines and related algorithms: A review" *Renewable and Sustainable Energy Review*, vol.13, pp.1-39, 2009.
- [5] A. Yazidi, H. Henao, G.A. Capolino, M. Artioli, and F. Filippetti, "Improvement of frequency resolution for three phase induction machine fault diagnosis," in *Record of IEEE Industry Applications Annual Meeting, 2005*, pp. 20-25.
- [6] A. Stefani, A. Yazidi, C. Rossi, F. Filippetti, D. Casadei, and G. A. Capolino, "Doubly fed induction machines diagnosis based on signature analysis of rotor modulating signals." *IEEE Trans. Ind. Appl.*, vol. 44, no. 6, pp. 1711–1721, Nov./Dec. 2008.
- [7] A. Stefani, F. Filippetti, and A. Bellini, "Diagnosis of induction machines in time-varying conditions," *IEEE Trans. Ind. Electron.*, vol. 56, no. 11, pp. 4548–4556, Nov. 2009.
- [8] S. H. Kia, H. Henao, and G. A. Capolino, "A high-resolution frequency estimation method for three-phase induction machine fault detection," *IEEE Trans. Ind. Electron.*, vol. 54, no. 4, pp. 2305–2314, Aug. 2007.
- [9] M. Pineda-Sanchez, M. Riera-Guasp, J. Roger-Folch, J. A. Antoninio-Daviu, J. Perez-Cruz, and R. Puche-Panadero, "Diagnosis of induction motor faults in time-varying conditions using the polynomial-phase transform of the current," *IEEE Trans. Ind. Electron.*, vol. 58, no. 4, pp. 1428–1439, Apr. 2011.
- [10] A. Garcia-Perez, R. de Jesus Romero-Troncoso, E. Cabal-Yepez, and R. A. Osornio-Rios, "The application of high-resolution spectral analysis for identifying multiple combined faults in induction motors," *IEEE Trans. Ind. Electron.*, vol. 58, no. 5, pp. 2002–2010, May 2011.
- [11] J. Cusido, L. Romeral, J. A. Ortega, J. A. Rosero, and A. G. Espinosa, "Fault detection in induction machines using power spectral density in wavelet decomposition," *IEEE Trans. Ind. Electron.*, vol. 55, no. 2, pp. 633–643, Feb. 2008.
- [12] I. P. Tsoumas, G. Georgoulas, E. D. Mitronikas, and A. N. Safacas, "Asynchronous machine rotor fault diagnosis technique using complex wavelets," *IEEE Trans. Energy Convers.*, vol. 23, no. 2, pp. 444–459, Jun. 2008.
- [13] S. Hedayati Kia, H. Henao, and G. A. Capolino, "Torsional vibration assessment using machine electromagnetic torque estimation," *IEEE Transactions on Industrial Electronics*, vol. 57, n° 1, pp. 209-219, Jan. 2010.
- [14] A. Bellini A. Yazidi, F. Filippetti , C. Rossi, and G. A. Capolino, "High frequency resolution techniques for rotor fault detection of induction machines," *IEEE Transactions on Industrial Electronics* , vol. 55, n° 12, pp. 4200-4208, Sept. 2008.
- [15] A. Bellini, F. Filippetti, C. Tassoni, and G.A. Capolino, "Advanced in diagnostic techniques for induction machines," *IEEE Transactions on Industrial Electronics*, vol. 55, n° 12, pp. 4109-4126, Sept. 2008
- [16] P. Caselitz, and J. Giebhardt, "Rotor condition monitoring for improved operation safety of offshore wind energy converters," in Proc. 2004 Conf. European Wind Energy Association, [Online]. Available:http://www.iset.unikassel.de/osmr/download/PaperEWEA_SP2004.pdf
- [17] Janning, J.; Schwery, A.; "Next generation variable speed pump-storage power stations," 13th European Conference on Power Electronics and Applications, 2009, pp.1-10, 2009